Rovibrational laser jet-cooled spectroscopy of SF_6-rare gas complexes in the v_3 region of SF_6

P. Asselin, A.C. Turner, Laurent Bruel, V. Brenner, M.-A. Gaveau, M. Mons

Rovibrational laser jet-cooled spectroscopy
of SF$_6$-rare gas complexes in the ν$_3$ region of SF$_6$

Pierre Asselin[a], Andrew C. Turner[b], Laurent Bruel[c], Marc-André Gaveau[d] and Michel Mons[d]

[a]*Sorbonne Université, CNRS, MONARIS, UMR 8233, 4 place Jussieu, Paris, F-75005 France.*
[b]*Department of Chemistry, University of Florida, Gainesville, Florida*
[c]*CEA Marcoule, DEN, Bagnols-sur-Cèze, France*
[d]*LIDYL, CEA, CNRS, Université Paris-Saclay, CEA Saclay 91191 Gif-sur-Yvette France*

Abstract

High resolution infrared spectroscopy combining an external cavity quantum cascade laser with a pulsed pin hole supersonic jet is used to investigate small van der Waals (vdW) hetero clusters containing SF$_6$ and rare gas (Rg) atoms in the ν$_3$ region of SF$_6$. In a first step, the rovibrational band contours of parallel and perpendicular transitions of 1:1 SF$_6$-Rg hetero dimers are simulated to derive ground and excited state parameters and hence S-Rg distances with a precision better than 0.5 Å. Due to the strong overlap of the SF$_6$-Ne spectrum by the intense SF$_6$ monomer one, the S-Ne distance could be only estimated from combining rules, which turned out to be very predictive for the other experimental S-Rg distances (deviation < ± 0.5%). In a second step, the signature of larger hetero clusters containing up to three Rg atoms is identified on the grounds of reduced red shifts of 1:2 and 1:3 complexes, normalized to the average red shift measured for the 1:1 complex. For the 1:1 and 1:2 complexes, reduced red shifts are shown to be nearly independent upon the Rg atom which suggests comparable structures in agreement with the C$_{3v}$ symmetry and confirms our assignments. Beyond the 1:2 complexes, the assignment of the two more red shifted remaining bands to 1:3 SF$_6$-Ar and SF$_6$:Kr hetero tetramers validates the red shift additivity rule up to three Rg atoms in the case of SF$_6$. Lastly, we evidence that the band shifts of the 1:1 SF$_6$-Rg hetero dimers can be correctly reproduced using a one-dimensional model for the intermolecular interaction based on the Buckingham potential which contains both long–range attractive and short-range contributions and enables to estimate the well depths of these vdW heterodimers.

I-   Introduction

Weak intermolecular forces such as van der Waals interactions play an important role in molecular sciences, ranging from the control of the conformational landscape of flexible biomolecules to the structure of molecular crystals.[1] These non covalent interactions are much weaker than the covalent bonds and even than the hydrogen bonds but the multicentric character of these interactions lead to a significant contribution which can affect the properties and structures of van der Waals (vdW) molecular complexes. High resolution spectroscopy has proved to be a suitable method to provide information on the structures and intermolecular interactions of these systems: in the microwave region several studies using molecular beam electric resonance[2] or pulsed nozzle Fourier transform techniques[3] enabled to characterize structure and internal dynamics in the ground state. In the near-UV region, laser induced fluorescence electronic spectroscopy has been used to provide a detailed description

of the solvation of aromatic molecules by rare gas atoms and document the role of vdW modes in molecular dynamics.[4]

The development of high resolution (HR) infrared (IR) spectroscopy in supersonic jets has allowed direct determinations of the potential energy surface (PES) of several diatomic (HF, HCl)[5,6,7,8] or linear triatomic molecules such as CO_2,[9,10,11] N_2O[12,13] and OCS[14,15] interacting with rare gases (Rg). The rovibrational analysis of such small complexes provided very precise structural parameters used to model the intermolecular PES. The dynamical picture is indeed more challenging in the case of floppy weakly bonded vdW Rg complexes with triatomic partners having large amplitude motions such as H_2O[16,17] and NH_3[18,19]: HR IR spectra of such complexes directly probe the rovibrational states related to a nearly flat PES with low energetic barriers. As a consequence, IR data are able to provide new insights into the state mixing of low lying vdW and internal rotor (H_2O) or umbrella inversion (NH_3) vibrational levels in the complex, the strength of the coupling between high intramolecular modes and these low frequency intermolecular vibrations, leading to a quantitative procedure for "deperturbing" the mixed states.[19]

Very few infrared studies were reported so far about mixed vdW clusters associating rare gases and large molecules.[20,21,22] Taking advantage of powerful line-tunable cw CO_2 lasers, Gough et al.[20] implemented infrared photofragmentation spectroscopy in molecular beams to study the low resolution IR spectrum of argon clusters seeded with a single SF_6 molecule in the spectral region of the triply degenerate v_3 vibration at 948 cm^{-1}. The v_3 band of SF_6 was found to shift monotonically to the red when increasing the backing pressure as a consequence of the increase of the average cluster size. Thereafter, Hartmann et al.[23] achieved the first high resolution laser spectroscopic study of vdW clusters of SF_6 and mixed SF_6-rare gas clusters in helium droplets at 0.37 K. The embedded complexes rotate nearly freely in liquid He as proved by the partially resolved rotational contours split into a parallel and a perpendicular band, but the increase (by more than a factor 3) in the moments of inertia of vdW complexes in He droplets leads to much smaller rotational constants than those of the free SF_6-Rg complex and consequently structural information transposable to the gas phase could be not extracted.

In a recent paper, we reported a high resolution infrared laser jet-cooled study of the SF_6 dimer and $(SF_6)_2$-Rg heterotrimers in the v_3 mode region.[24] Taking advantage of our versatile set-up, various experimental conditions of nozzle geometry, axial distance and SF_6 concentration were explored to revisit the conformational landscape of the SF_6 dimer. Two conformers were unambiguously identified on the grounds of rovibrational analysis of the parallel band contours of the v_3 transition. For each conformer a specific dynamics of formation was evidenced from the evolution of their relative populations along cold/fast and hot/slow expansions. Besides that, the spectroscopic evidence of $(SF_6)_2$-Rg heterotrimers built from the least stable $(SF_6)_2$ conformer suggested the picture of an entropically favored second dimer, favoured by the presence of a rare gas collision partner, and separated from the most stable conformer by a low barrier.

The second part of the study, presented hereafter, is dedicated to the spectroscopic characterization of 1:1 SF_6-Rg heterodimers in the v_3 mode region using the infrared tunable laser spectrometer recently implemented in our laboratory, which combines a pulsed

supersonic jet with an external cavity quantum cascade laser (EC-QCL) in the 10.5 µm region. The high resolution rovibrational spectra of parallel and perpendicular bands of SF_6-Rg complexes enable us to extract precise S-Rg bond lengths and band origin shifts. These experimental data are then used to parameterize a simple model for the intermolecular potential. Lastly, vibrational signatures assigned to larger clusters up to SF_6-$(Rg)_3$ on the red side of the 1:1 heterodimer constitute an interesting benchmark to test the evolution of the red shift with the cluster size at least for the first solvation steps .

II- Experimental details

The vibration-rotation spectra of SF_6-rare gas clusters have been recorded using an external-cavity quantum cascade laser (EC-QCL) coupled to a pulsed supersonic jet. This set-up has been already described in previous papers[24,25] and only the main characteristics will be described in the present study.

The light source is a continuous-wave room-temperature mode-hop-free EC-QCL with a spectral width of 10 MHz, which covers the 930-990 cm^{-1} range (Daylight Solutions). About 8% of the total light is sent through two laser channels for relative and absolute frequency calibrations. Relative frequencies are monitored by measuring the intensity transmitted through a solid germanium etalon with a free spectral range of 490 MHz, to provide a relative frequency scale. Absolute laser frequencies are obtained by measuring the transmission through a 15 cm-length reference cell containing a known reference gas at a pressure of about 5 mbar (ethene in the present work). The remaining light is sent through a multipass optical cavity mounted in the jet chamber, which is evacuated by a 2000 l/s oil diffusion pump backed by a combination of a 350 m^3/h Roots blower and a 40 m^3/h rotary pump. The cavity composed of two 1.5" astigmatic mirrors (R=99.2 %, AMAC-36, Aerodyne Research) is aligned according to a 182-pass pattern which crosses almost perpendicularly the jet expansion. Three liquid-nitrogen-cooled HgCdTe detectors (Judson J15D12) are used to measure the powers transmitted through the multipass cavity, the etalon and the reference gas cell. In our recent study about pure $(SF_6)_2$ and mixed $(SF_6)_2$-rare gas clusters,[24] molecular complexes were stabilized whatever the geometry of the supersonic expansion used, either planar or axisymmetric, which enabled to change the rotational temperature and to promote one conformer with respect to another. In the present work, the (SF_6)-Rg complexes were investigated in the same manner from the expansion of a molecular jet at very high dilution of the SF_6/Rg mixture seeded in helium backing pressures as high as 8 bar. Two nozzle geometries were tested: either a pulsed circular nozzle (General Valve Series 9) in standard configuration with a 0.35 mm diameter (D) pin hole or by fitting the pin hole nozzle with two modified industrial blades, forming a 30 mm length x 50 µm width (l) slit opening. Van der Waals heterodimers were stabilized at rotational temperatures T_R below 1 K and then probed by the infrared laser light at z average distances between 9 and 18 mm from the nozzle exit. The z values are only indicative because the zone Δz probed in the jet by the optical cavity covers several mm and corresponds to a range of reduced distances z/D between 25 and 50. A good balance between efficient rovibrational cooling and high molecular density was found at about z = 15 mm for the present pin hole jet expansions.

Our rapid scan scheme is similar to previous designs developed for high resolution molecular spectroscopy.[26] Spectra are recorded by driving the piezoelectric transducer of the

EC-QCL diffraction grating with a 100 Hz sine wave. This allows the QCL frequency to be scanned once per period over 0.8 cm^{-1} in 5 ms. During this time window, the intensities transmitted through the supersonic jet, the etalon and the reference gas cell are digitized and recorded simultaneously as a function of time. A baseline-free transmittance through the multipass cavity is obtained by taking the ratio of signals recorded in presence and absence of the jet (by opening or not the nozzle). The procedure for absolute frequency calibration is achieved *a posteriori* by measuring the deviation between experimental and HITRAN12 database C_2H_4 frequencies to correct the free spectral range value of the etalon fixed at the beginning of each experiment. The accuracy of the frequency calibration is around 0.0005 cm^{-1}.

III Experimental results

On the grounds of scarce previous high resolution infrared experiments about SF_6-Rg clusters,[20,23] rovibrational signatures have been searched on the red side of the ν_3 band origin of SF_6 monomer using SF_6/Rg equimolar mixtures and different dilutions of SF_6 in He at backing pressures of 8 bar. In a first series of experiments, a slit nozzle was used, knowing that $(SF_6)_2$ and $(SF_6)_2$-Rg clusters were easily detected in planar expansions with weaker Doppler broadenings than with a pin hole jet.[24] However, no SF_6-Rg complex absorption could be detected with the slit nozzle whatever the dilution used. Owing to the high temperatures of the planar expansions compared to axisymmetric ones, as illustrated by the previously measured rotational temperatures for $(SF_6)_2$,[24] 3 K and 0.8 K in these respective expansions for comparable generating conditions, the absence of 1:1 complex signal in the planar expansions should be ascribed to a lower stability of the 1:1 complex compared to the homodimer.A second series of experiments realized with the pin hole nozzle enabled us to observe new bands on the red side of the ν_3 band of SF_6 monomer, which are assigned to SF_6-Rg (Rg = Ne, Ar, Kr, Xe) 1:1 clusters. This absorption signal was maximized by tuning the dilution of the SF_6/Rg mixture to 1/8 for heavier rare gases and 1/100 for Ne. Due to the very close presence of the intense ν_3 band of SF_6 monomer, jet-cooled spectra of SF_6 monomer were recorded with the same SF_6/He dilution as that used in overlapped SF_6-Rg and SF_6 spectra with SF_6/Rg/He ternary mixtures, and then subtracted to isolate the contribution of the vdW SF_6-Rg heterodimer. Figure 1 displays the example of the SF_6-Ar spectrum, exhibiting a large contribution of the SF_6 monomer ν_3 band which can be efficiently removed following this subtraction. Figure 2 displays the four EC-QCL jet-cooled spectra of SF_6-Rg for Rg = Ne, Ar, Kr and Xe after subtraction.

Rotational analyses

As for the SF_6 dimer study[24], it is expected to observe parallel and perpendicular bands of SF_6-Rg arising from the reduction of degeneracy of the triply degenerate state (ν_3) of the SF_6 monomer in complexes of C_{3v} symmetry.
Q-branch maxima of parallel bands for SF_6-Ar, SF_6-Kr and SF_6-Xe are clearly visible (Fig. 2) at 946.977, 946.638 and 946.221 cm^{-1}, respectively with well resolved P- and R-branch structures. The K structure is not resolved within our experimental linewidth (150 MHz), limited by residual collisional and Doppler broadenings. For the three heaviest rare gases, Q-

branch maxima of SF_6-Rg bands exhibit increasing red shift with respect to the v_3 band of SF_6, reaching up to about 1.8 cm^{-1} for SF_6-Xe. With Ne, the red shift is so weak that several features of the SF_6-Ne spectrum are overlapped with intense P branch lines of the SF_6 monomer band, which prevented any rovibrational analysis. A sharp maximum is observed at about 947.86 cm^{-1} but no splitting between parallel and perpendicular bands could be evidenced in agreement with the helium droplet study[23].

All perpendicular bands display characteristic $^{P,R}Q(J,K)$ branches, in particular very strong $^RQ(J,0)$ ones at 947.392, 947.175 and 946.897 cm^{-1} for SF_6-Ar, SF_6-Kr and SF_6-Xe, respectively and broader $^PQ(J,K>0)$ and $^RQ(J,K>0)$ branches, observed on both sides of $^RQ(J,0)$. Similarly to the perpendicular band of the SF_6 dimer, SF_6-Kr and SF_6-Xe complexes display a first-order Coriolis interaction, as proved by experimental spacings between nearby Q branch peaks, which are close to the calculated value of $2(A(1-\xi)-B) \approx 0.027$ cm^{-1} for SF_6-Kr and 0.034 cm^{-1} for SF_6-Xe, by taking the Coriolis parameter ξ of the SF_6 monomer, equal to 0.69374,.[27]

From the perpendicular band contour of SF_6-Ar, the first-order Coriolis interaction is more difficult to evidence : very few intense $^RQ(J,K>0)$ branch peaks at 947.409, 947.422 and 947.435 cm^{-1} are found to be spaced by 0.013 cm^{-1} in agreement with the calculated spacing value while $^PQ(J,K>0)$ branch peaks are too weak to be observed. Besides that, a series of intense features is observed on the R branch side with a spacing between 0.0055 and 0.063 cm^{-1} and could belong to $^RR(J,K)$ or $^PR(J,K)$ lines.

Our experiments confirm the reduction of degeneracy of the triply degenerate state (v_3) of the SF_6 monomer with a first-order Coriolis interaction, into A and E states in complexes of C_{3v} symmetry. Band contour analyses are proceeded in two steps: firstly, the simulations of three parallel bands of SF_6-Ar, SF_6-Kr and SF_6-Xe (Figure 3) were realized according a symmetric top structure to derive best fit molecular parameters $v_{//}$, A', B'' and B'. The ground state experimental rotational constants were used to obtain accurate experimental S-Rg distances (Table 1), assuming an unchanged monomer structure upon heterodimer formation. Secondly, perpendicular bands were simulated by fixing A'' to the ab initio value and B'' to the value derived from the parallel band contour simulation to obtain the best fit molecular parameters A', B', $v_\perp$ and ξ. Figure 4 displays the comparison between both jet-cooled perpendicular band spectra of SF_6-Kr and SF_6-Xe and our best simulations, while the observed perpendicular band of SF_6-Ar could not be correctly fitted. The too few intense $^RQ(J,K>0)$ branch peaks prevented us to start properly the rovibrational analysis. Table 1 reports the sets of molecular parameters derived from these band contour analyses. The transition frequencies of parallel and perpendicular bands of the SF_6-Rg heterodimers are listed in the Table 1 of Supplementary Material File (SMF).

Spectral shifts

Lastly, ten additional weak bands are observed: at 946.693, 946.483, 946.220 and 945.664 cm^{-1} in the SF_6-Ar spectrum, at 946.241, 945.938, 945.612 and 945.320 cm^{-1} in the SF_6-Kr spectrum and at 945.857 and 945.371 cm^{-1} in the SF_6-Xe spectrum on the red side of both parallel and perpendicular bands of heterodimers (indicated by stars in Figure 2). The corresponding red shifts range between 1 and 3 cm^{-1}, which is consistent with the signature of

larger heteroclusters containing up to three Rg atoms, assuming a red shift additivity rule. In addition, since the larger complexes are expected to exhibit a complete lifting of ν_3 vibration, a set of three bands can be anticipated for each of them, leading to an increased complexity of the spectral pattern. In order to assign the spectra and assess their robustness relative to the nature of the rare gas, reduced red shifts have been considered (Table 2), i.e., red shifts normalized to the average red shift measured for the corresponding 1:1 complex, which is defined as :

$$\Delta\nu_{1:1} \ = \ (\Delta\nu_{//} + 2\Delta\nu_{\perp})/3 \tag{1}$$

where $\Delta\nu_{//}$ and $\Delta\nu_{\perp}$ correspond to the red shift of parallel and perpendicular bands, respectively.

For the 1:1 complexes, the reduced shifts of the perpendicular and parallel bands are nearly independent upon the nature of the rare gas, with values close to 0.81 and 1.36 respectively. This suggests comparable structures for this complex, in agreement with the C_{3v} symmetry anticipated, due to three simultaneous F-Rg close contacts, made possible by the similar van der Waals radii of F and the rare gas atoms. Interestingly, the three next reduced shifts obtained along the series of Ar, Kr and Xe rare gases beyond the 1:1 complex also turn out nearly independent upon the nature of the rare gas, with values close to 1.7, 2.0 and 2.4, and an average value of about 2.0.

These observations are fully consistent with i) the assignment of these three bands to the 3 components of the ν_3 vibration in a 1:2 complex, ii) the validity of the shift additivity rule, and iii) a structure independent upon the rare gas. For the next bands observed (case of Ar and Kr), the reduced shifts being in the vicinity of 3, they are assigned to a 1:3 complex. However the different values suggests that they correspond to different components of the ν_3 vibration

IV Discussion

Comparison between experimental and theoretical structural parameters

The ground state rotational constants derived from the present high resolution infrared study provide reliable intermolecular distances d(SF_6-Rg) (Table 1) with an accuracy ranging between 0.15 pm for SF_6-Xe and 0.5 pm for SF_6-Ar. It is worth to compare these experimental distances with both ab initio calculations and simple theoretical models to evaluate the predictive character of these methods.

In order to account for the dispersive character of the vdW SF_6-Rg interactions, geometry optimizations have been carried out using the density functional theory corrected by explicit dispersion terms (DFT-D), at the RI-B97-D/def2-TZVPPD level of theory with the D3 type Grimme correction (including the Becke-Johnson damping and three-body terms), and using an adapted pseudo potential (effective core potential) for Xe.[28] All calculations were carried out using the TurboMole[29] package. This method was first validated on purely dispersive Rg-Rg dimers, as a test case before applying it to SF_6-Rg systems. Relative discrepancies between 3 and 7 % were obtained, always with a surestimation of the Rg-Rg distances, compared to experimental data derived from various fitting procedures.[30,31,32,33] Geometry optimizations of SF_6-Rg complexes without constraints (C_{3v} geometry

corresponding to saddle points) or not (minimum) give relative errors comparable to rare gas dimers. Such calculations are currently optimizing geometries in the bottom of the potential well and vibrational averaging effects in the ground state (zero point energy or ZPE) expected to be notable in a nearly flat vdW well are not taken into account.

The S-Rg distances can be also predicted from the combining rules,[34,35] currently used to derive the vdW Lennard-Jones well depths and equilibrium interatomic distances $d(SF_6-Rg)$ of SF_6-Rg heterodimers from the distances $d(SF_6-SF_6)$ of $(SF_6)_2$ and $d(Rg-Rg)$ of $(Rg)_2$ homodimers. For our comparisons, we choose the arithmetic mean rule[34] where the distance of unlike molecules is obtained by addition of the vdW radii i.e. $d(SF_6-Rg)=$ $[d(SF_6-SF_6)+ d(Rg-Rg)]/2$. The $d(SF_6-SF_6)$ value of 470.5 pm obtained by Aziz at al.[36] from virial data, viscosity and a potential Morse-Morse-Spline-van der Waals (MMSV) and the $d(Rg-Rg)$ distances experimentally determined by the fit of literature data have been used.[30-33]

Table 3 gathers the $d(SF_6-Rg)$ intermolecular distances obtained from the high resolution infrared jet-cooled study compared to RI-DFT-D calculations and combination rules. A systematic error around 5 % is obtained for theoretical intermolecular distances, as a consequence of the underestimation of the computed B" ground state rotational constant. On the other hand, a remarkable agreement is observed with distances derived from combining rules (± 0.5 % deviation with respect to the experimental ones) Such a good predictive method gives confidence to estimate the SF_6-Ne distance which could not be derived from the rovibrational analysis, and turns out to be useful in the intermolecular part of the discussion. In the following, we will exploit intermolecular distances and parallel and perpendicular experimental shifts derived from the present high resolution jet-cooled infrared study to determine the most appropriate model of intermolecular potential for SF_6-Rg.

Signature of larger SF_6-Rg$_{2,3}$ heteroclusters

Relative red shifts reported in Table 2 suggest three remarks: (i) the spectra of several rare gases obey very similar patterns with close relative weights between parallel and perpendicular shifts for SF_6-Rg and $-Rg_2$. This result gives confidence for our assignments of heteroclusters up to n=2. (ii) beyond the SF_6-Rg$_2$ signatures, the two remaining bands are assigned to SF_6-Ar$_3$ and SF_6-Kr$_3$ hetero tetramers. Their relative shift with the rare gas is around 3 but displays a relative difference of about 15 % which suggested that these bands do not belong to the same symmetry, (iii) the red shift additivity rule holds very well in the case of SF_6-Rg$_n$ heteroclusters up to n=3.

These measurements are remarkably consistent with an additivity of vibrational shifts when increasing the number of Rg atoms. Moreover, the experimental frequency shift of 0.72 cm^{-1} per argon atom well agrees with that roughly derived from photofragmentation experiments[20] which measured a total shift of 7 cm^{-1} for SF_6-Ar$_n$ distributed between n = 1 and 12, that is an average shift of 0.6 cm^{-1} per argon by assuming the additivity of shifts.

Intermolecular potential for SF_6-Rg

Theoretical models were developed in the past to predict the frequency shifts of complexes between molecules of high symmetry (SiF$_4$, SF$_6$) and rare gases.[21,37,38]. For such systems, the dominant contribution of the band shift was found to be the dipole-induced

dipole mechanism as a consequence of the influence of the Rg atom.[37] As for the SF_6 dimer but with a corresponding shift about fifteen times weaker, this perturbation splits the triply degenerate ν_3 band of the free SF_6 molecule due to the vibrational dipole moment parallel (*A* symmetry) and perpendicular (*E* symmetry) to the bond axis of the complex into two $\nu_{//}$ and doubly degenerate $\nu_\perp$ components.

The frequency shifts following this model can be expressed by :

$$\Delta\nu_{\perp th} = -\Delta E_{ind}/hc \quad \text{and} \quad \Delta\nu_{//th} = 4\Delta\nu_{\perp th} \tag{2}$$

$$\text{with} \qquad \Delta E_{ind} = \frac{\hbar\alpha}{2\omega_3 R^6}\left(\frac{\partial\mu}{\partial Q_3}\right)^2 \tag{3}$$

where α is the polarizability of the rare gas atom, ω_3 is vibrational frequency of the ν_3 band of SF_6, R is the S-Rg distance and $\frac{\partial\mu}{\partial Q_3}$ is proportional to the vibrational transition dipole moment of the ν_3 mode of SF_6. The same expression (Eq.1) holds for the calculated frequency shift $\Delta\nu_{th}$ as for the experimental one, and finally, one obtains from Eqs (1-2) $\Delta\nu_{th} = 2\Delta\nu_{\perp th}$ whose numerical values for SF_6-Ar, -Kr and –Xe are reported in Table 2. As can be seen in this table the calculated shifts for the SF_6-Rg heterodimers are largely underestimated (by more than 50 %) with respect to the experimental ones, while the ratios of the shifts ($\Delta\nu_\perp/\Delta\nu_{//}$) between *E* and *A* states, predicted to be 0.25 (Eq. 2), are measured between 0.585 for SF_6-Ar and 0.615 for SF_6-Xe. Otherwise, the dependence between the experimental shift $\Delta\nu_{exp}$ and the ΔE_{ind} term of pure induction potential varying with $\frac{\alpha}{R^6}$ strongly deviates from linearity which confirms that this model fails to reproduce the observables.

Another approach is to consider that the most important effects of vibrational excitation on the high symmetry SF_6 molecule can be modeled using the radial Buckingham potential.[39] Guided by previous studies on linear molecules (N_2O, CO_2 and OCS) in interaction with rare gases[9,10,15] we assumed that the most important shift effects can be controlled by the repulsive A and β, and attractive C_6 parameters, according to the form

$$V(R) = Ae^{-\beta R} - C_6/R^6 \tag{4}$$

Upon complexation with Ne, Ar, Kr and Xe, the band origin of the stretch of the SF_6 monomer was observed to shift by $\Delta\nu_{exp}$ derived from Eq.(1), equal to -0.117, -0.723, -0.981 and -1.305 cm^{-1}, respectively. This red (bathochromic) shift is an indication of an increase of the intermolecular potential well depth between the ground and excited states.

In this model, the intermolecular distance at the minimum R_m obeys the following relationship

$$\beta Ae^{-\beta R_m} = 6C_6/R_m^7 \tag{5}$$

and a well depth ε at the minimum (ε>0) given by

$$\mathcal{E} = \frac{C_6}{R_m^6}(1 - 6/\beta R_m) \tag{6}$$

Vibrational excitation induces a change of the repulsive and attractive parameters, ΔC_6 and ΔA respectively, while the change in repulsive parameter β is assumed to be negligible. Under these assumptions, the change in the position of the radial minimum is obtained by differentiating Eqs (5) and (6) and can be expressed under the form

$$\Delta R_m = (\frac{\Delta A}{A} - \frac{\Delta C_6}{C_6})/(\beta - 7/R_m) \tag{7}$$

The resulting change in the well depth is given by

$$(\Delta\mathcal{E}/\mathcal{E}) = \left(\frac{\beta R_m}{\beta R_m - 6}\right)\left[\frac{\Delta C_6}{C_6} - \left(\frac{\Delta A}{A}\right)\frac{6}{\beta R_m}\right] \tag{8}$$

In the case where the variations of ZPE due to vdW vibrations are negligible, $\Delta\mathcal{E}$ can be replaced by $-\Delta\nu_{exp}$. From Eq.(8), it appears that the fractional change in the well depth is a delicate balance between the change in attractive and repulsive contributions.

An important question is to determine how these terms vary for the series of the SF_6-Rg complexes observed. On one hand, the long range attractive forces scale with the polarizability α of the Rg atom which defines the usual order of well depths from Ne to Xe. On vibrational excitation of SF_6, only the properties of SF_6 change and it is expected that the fractional change in attraction $\Delta C_6/C_6$ will also scales with α and should be independent of the nature of the Rg atom. On the other hand, the repulsive forces between the Rg atom and each of the atoms of SF_6 are modulated by the individual motions of the atoms in SF_6. The change in the repulsion term $\frac{\Delta A}{A}$ can be approximated to $(\beta^2/2)\Delta x^2$ where x is the relative displacement of individual atoms in the SF_6 molecule while Δx^2 represents the change in the square of the amplitude of vibrational motion and should be identical for all the complexes of the same series. Hence $\frac{\Delta A}{A}$ at given R_m just depends on β^2. Eq.(8) becomes:

$$\Delta\nu_{exp} (R_m^6/C_6) = (3\beta/R_m)\Delta x^2 - \Delta C_6/C_6 \tag{9}$$

Owing to the same expected values of Δx^2 and $\Delta C_6/C_6$ for the series of SF_6-Rg complexes we should observe a linear dependence in (Eq. 9) between the terms $\Delta\nu_{exp} (R_m^6/C_6)$ and $(3\beta/R_m)$. To check it we need to quantify the repulsive parameter β and the vdW coefficient C_6 for all SF_6-Rg heterodimers. It has been shown that β depends quantitatively upon the tail of the wavefunctions of the interacting molecules. From quantum defect theory,[40] the asymptotic form of the wavefunction depends upon the ionization energy of the molecule and takes the form

9

$$\Psi \ \alpha \ e^{-R/a_0 n_{eff}} \hspace{4cm} (10)$$

where a_0 is the Bohr radius and n_{eff} is an effective principal quantum number such that $n_{eff}^2 = R_d/E_i$ (R_d Rydberg constant, E_i ionization energy). By analogy with the asymptotic form of the repulsion, it comes

$$\beta = (1/n_{eff,SF_6} + 1/n_{eff,Rg})/a_0 \hspace{3cm} (11)$$

The values of β for SF_6-Rg obtained with Eq.(11) are derived from effective principle quantum numbers calculed from ionization potential values[41] and are reported in Table 2 of SMF. Two types of C_6^{AB} coefficients for AB heterodimers could be extracted from the literature: (i) directly from measurements of the total differential cross sections in crossed molecular beams or calculations from experimental frequency-dependent polarizabilities by Pack et al.[42,43] (ii) indirectly using the combining rule $C_6^{AB} \approx (C_6^{AA} C_6^{BB})^{1/2}$ expected to be a good approximation.[36]**Erreur ! Signet non défini.** After examination of available data, C_6^{AB} coefficients obtained experimentally are discarded owing to a large and rare gas-dependent uncertainty. C_6^{Rg-Rg} and $C_6^{SF_6-SF_6}$ calculated coefficients from recognized works of Tao et al.[44], Vydrov et al.[45] and Kumar et al.[46] are used to obtain good estimates of $C_6^{SF_6-Rg}$ with a small deviation and are reported in Table 2 of SMF.

Table 4 gathers all the parameters required to plot the graph $\Delta\nu_{exp}$ (R_m^6/C_6) as a function of $(3\beta/R_m)$. The plot of the SF_6-Rg series is displayed in Fig. 5. The linear dependence is clearly observed with a standard deviation of 2×10^{-4}.

The linear fit provides a slope Δx^2 equal to 0.00521(28) and an intercept $\Delta C_6/C_6$ equal to 0.01914(82). The well depth ε of these complexes can be properly estimated by the theory from Eq.(6) (Table 4). Returning to the expression for the band origin shift in Eq(8) attractive and repulsive contributions can now be evaluated. βR_m is equal to about 17.2(2) whatever the Rg atom and the factor $\left(\frac{\beta R_m}{\beta R_m - 6}\right)$ is close to 1.53(1). From the extrapolation of the linear fit, the contribution of the attraction alone is about 3 %, independently of the Rg atom which would produce red shifts between 3 and 7 cm^{-1} from Ne to Xe. The small values of the observed red shifts (between 0.1 and 1.3 cm^{-1}) are a direct consequence of the repulsion. The repulsive term $3\beta/R_m$ (ranged between 3.4 and 2.5 from Ne to Xe) fully compensates the attractive one for Δx^2 values between 0.0056 and 0.0076 Å^2.

Conclusion

In the following of a recent high resolution rovibrational low temperature study providing new insights about the conformational landscape of SF_6 dimer and its complexation with rare gas atoms, the present work is devoted to the characterization of the series of 1:1 SF_6-Rg (Rg = Ne, Ar, Kr, Xe) heterodimers in the region of the ν_3 band of SF_6 monomer using the infrared tunable quantum cascade laser spectrometer coupled to a pulsed supersonic jet developed in Monaris. Accurate S-Rg distances for Rg = Ar, Kr , Xe were derived from the rovibrational analysis of parallel band contours of the ν_3 transition. For these 1:1

complexes, the reduced shifts of parallel and perpendicular bands almost unchanged whatever the rare gas, suggest similar structures in agreement with the C_{3v} symmetry anticipated. The observed signatures of larger heteroclusters containing up to three Rg atoms, fully validate the shift additivity rule for the first solvation steps and a structure independent upon the rare gas for the three bands of the 1:2 complex. Lastly, the frequency shifts values of 1:1 SF_6-Rg heterodimers nicely proved to be quite compatible with the model of a radial Buckingham PES controlled by a fine equilibrium between attractive and repulsive contributions. Upon complexation of SF_6 with a rare gas atom, the red shifts measured are indicative of an increase of the well depths between ground and excited states, whose absolute values were estimated from the Buckingham model, between 1 kJ/mol (Ne) up to almost 3 kJ/mol (Xe).
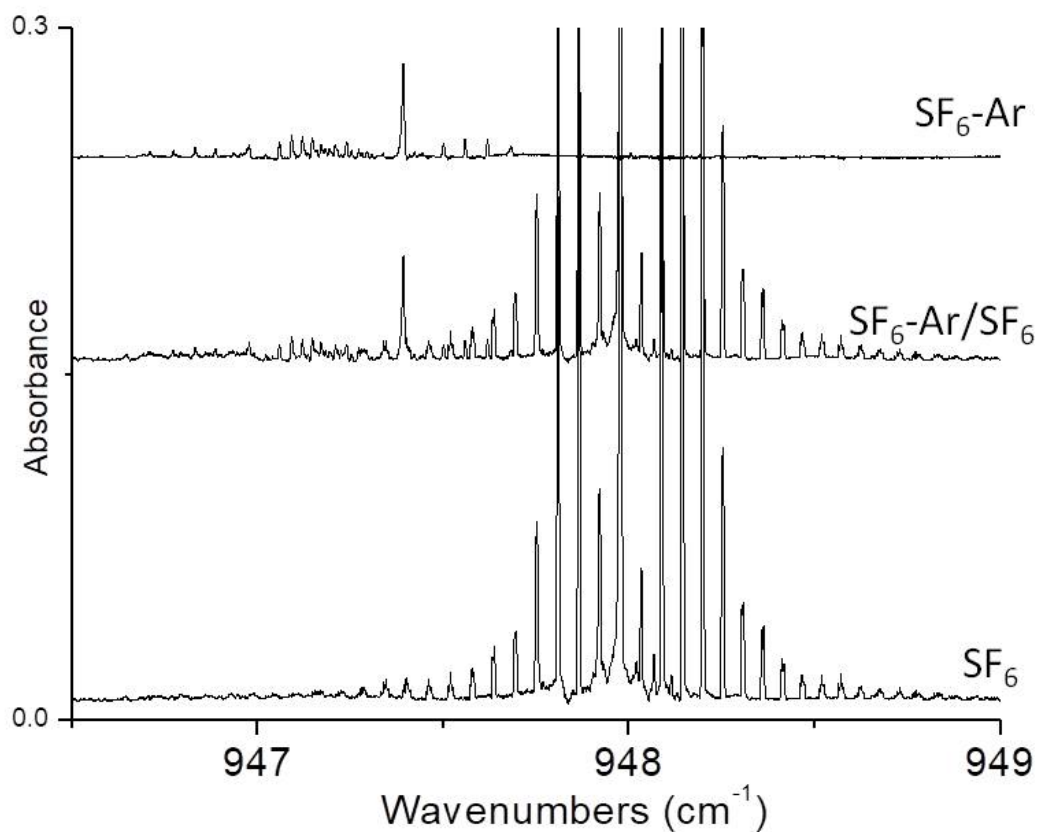
Fig.1 EC-QCL jet cooled spectra of the ν_3 band of SF_6 monomer for 0.12 % SF_6 (bottom), and for 0.12% SF_6 and 1% Ar (middle) diluted in 8 bar helium at an axial distance $z = 15$ mm for the pin hole nozzle. The spectrum of SF_6-Ar obtained after subtraction of both jet-cooled spectra is displayed above.

Fig.2 EC-QCL jet cooled spectra of SF_6/Rg/He mixtures diluted in 8 bar helium at an axial distance $z = 15$ mm for the pin hole nozzle, after subtraction of the spectrum of SF_6 monomer recorded in the same conditions of dilution of the SF_6/He mixture. The SF_6/Rg/He mixtures used are 0.12/1/100 for SF_6-Rg with Rg = Ar, Kr, Xe and 0.18/18/100 for SF_6-Ne. The bands marked by stars have been assigned to larger SF_6-$(Rg)_{2-3}$ heteroclusters.

Fig. 3: EC-QCL jet cooled pin hole spectra of both ν_3 parallel bands of SF_6-Rg heterodimers (Rg=Ar, Kr, Xe) with 0.12 % SF_6 and 1% Rg diluted in 8 bar helium at an axial distance $z = 15$ mm, compared to our best simulation. The rotational temperature used for these simulations is 0.7(1) K.
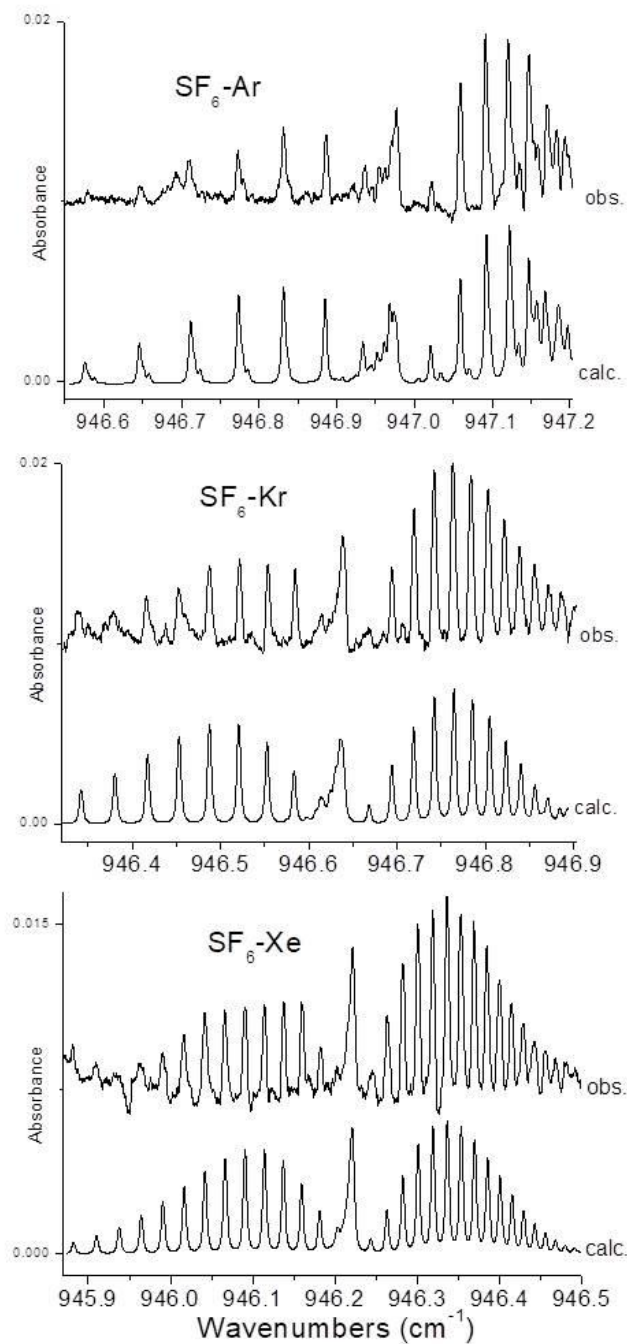
Fig. 4: EC-QCL jet cooled pin hole spectra of both ν_3 perpendicular bands of SF_6-Rg heterodimers (Rg= Kr, Xe) with 0.12 % SF_6 and 1% Rg diluted in 8 bar helium at an axial distance z = 15 mm, compared to our best simulation. The rotational temperature used for these simulations is 0.7(1) K.
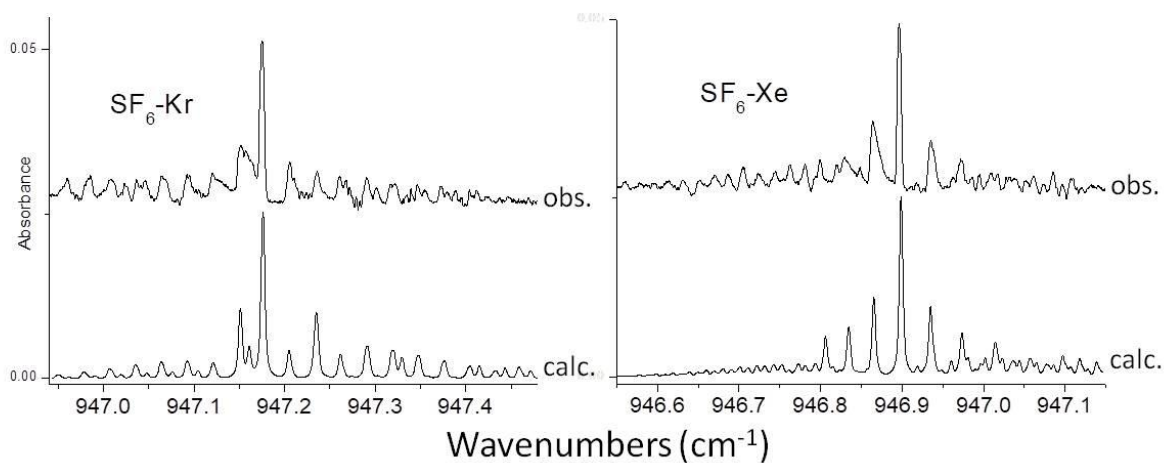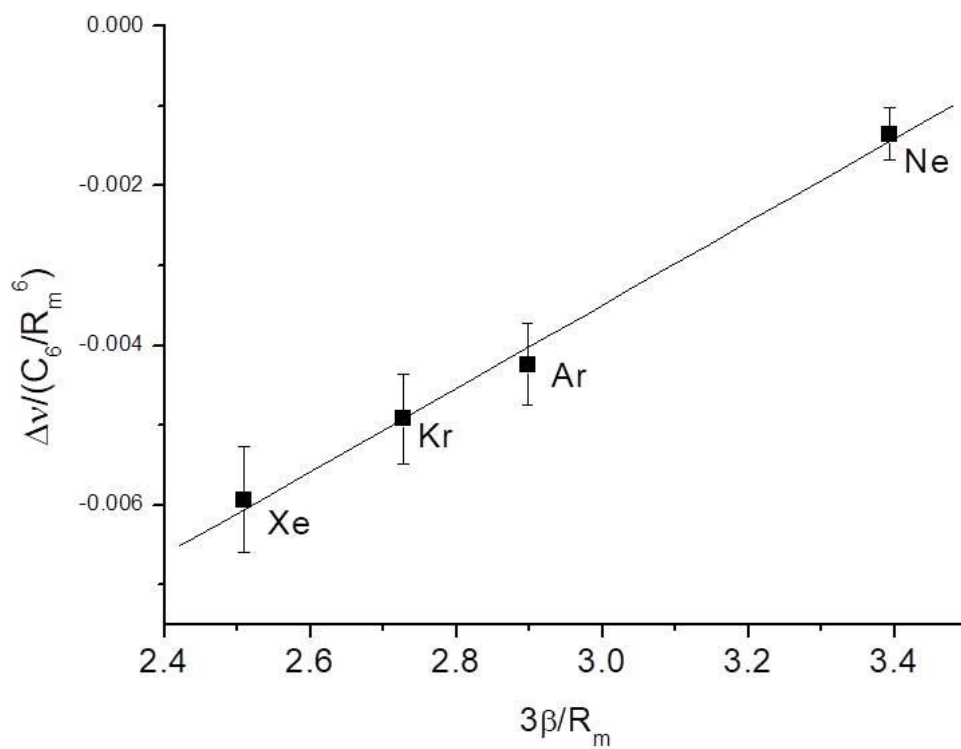
15

Figure 5: Relation shift between Δv_{exp} (R_m^6/C_6) and ($3\beta/R_m$) for the complexes SF_6-Rg based on the model of the Buckingham intermolecular potential.

	SF$_6$-Xe	SF$_6$-Kr	SF$_6$-Ar
	Parallel band		
A''/cm^{-1}	0.0874[a]	0.0874[a]	0.0874[a]
B''/cm^{-1}	0.010382(6)	0.014158(17)	0.022765(45)
A'/cm^{-1}	0.087261(35)	0.086956(59)	0.086804(85)
B'/cm^{-1}	0.010102(6)	0.013535(14)	0.020733(36)
ν_0/cm^{-1}	946.22327(18)	946.64108(30)	946.97950(48)
d(SF$_6$–Rg)/pm	456.17(15)	434.60(27)	420.82(50)
	Perpendicular band		
A''/cm^{-1}	0.0874[a]	0.0874[a]	0.0874[a]
B''/cm^{-1}	0.010382[b]	0.014158[b]	0.022765[b]
A' /cm^{-1}	0.08865(17)	0.10471(14)	-
B'/cm^{-1}	0.010395(7)	0.014296(13)	-
ν_0/cm^{-1}	946.94171(37)	947.22478(39)	947.392[c]
ξ	0.687(2)	0.663(2)	

[a] RI-DFT-D ab initio value of A''.
[b] Ground state B'' constants for the perpendicular band analyses are fixed to the B'' values derived from the parallel band analyses.
[c] The ν_0 frequency for the perpendicular band of SF$_6$-Ar corresponds to the maximum of the $^R Q(J,0)$ branch.

Table 1: Molecular parameters (rotational constants, band centers and S-Rg distances) for the ground and ν_3 parallel and perpendicular states of the van der Waals SF$_6$-Rg heterodimers (Rg= Ar, Kr, Xe) derived from the band contour analyses of EC-QCL jet-cooled pin hole spectra.

	SF$_6$-Rg				SF$_6$-Rg$_2$				SF$_6$-Rg$_3$	
red shifts (cm^{-1})	$\Delta\nu_\perp$	$\Delta\nu_{//}$	**$\Delta\nu_{exp}$**	$\Delta\nu_{th}$	$\Delta\nu_1$	$\Delta\nu_2$	$\Delta\nu_3$	**$\Delta\nu_{exp}$**	$\Delta\nu_1$	$\Delta\nu_2$
Ne			0.117[a]							
Ar	0.585	1.000	**0.723**	*0.448*	1.284	1.494	1.755	***1.511***	-	2.313
Kr	0.802	1.339	**0.981**	*0.570*	1.736	2.045	2.365	***2.049***	2.657	-
Xe	1.08	1.756	**1.305**	*0.694*	2.120	2.607		***-***		
relative red shifts	*$\Delta\nu_\perp$*	*$\Delta\nu_{//}$*	***$\Delta\nu_{exp}$***		$\Delta\nu_1$	$\Delta\nu_2$	$\Delta\nu_3$	**$\Delta\nu_{exp}$**	$\Delta\nu_1$	$\Delta\nu_2$
Ne										
Ar	0.809	1.383	**1**		1.776	2.067	2.427	***2.090***	--	3.199
Kr	0.818	1.365	**1**		1.770	2.085	2.411	***2.088***	2.708	
Xe	0.828	1.346	**1**		1.625	1.998	--			

Table 2: Experimental ν_3 red shifts (*upper panel*) observed for the parallel and perpendicular bands of the SF$_6$-Rg dimer and the three bands of the SF$_6$-Rg$_n$ heteroclusters in the series of EC-QCL jet-cooled pinhole spectra. For each rare gas, the experimental shifts $\Delta\nu_{exp}$ (calculated according to relations (1) and (2)), are compared to the theoretical shifts ($\Delta\nu_{th}$) derived from a pure induction model[37] given in italics; *lower panel*: relative red shifts after normalization by the experimental red shift $\Delta\nu_{exp}$, of the 1:1 complex, showing that the spectra of the several rare gases obey very similar patterns.

	Exp.	Calc. (RI-DFT-D)			Error (%) Calc./Exp.	Combination rules (CR)	Error(%) CR/Exp
		Minimum	C_{3v} constrained	Factor scaling 0.95			
Ne-Ne	309.1[a]						
Ar-Ar	375.7[a]	401	-		+ 6.7		
Kr-Kr	401.1[a]	413.5	-		+ 3.1		
Xe-Xe	436.6[a]	456.6	-		+ 4.6		
SF_6-Ne		426.0	420.9	404.7		389.8	-
SF_6-Ar	420.82[b]	441.7	440.3	419.6	+ 5.0	423.1	+ 0.6
SF_6-Kr	434.60[b]	455.7	458.0	432.9	+ 4.9	435.8	+ 0.3
SF_6-Xe	456.17[b]	475.8	471.6	452.0	+ 4.3	453.6	- 0.5

[a]Interatomic distances of rare gas dimers derived from the interatomic potential built by fitting empirically experimental data (Aziz et al.)[30-33]

[b] present data

Table 3: Comparison between experimental SF_6-Rg distances obtained from the present high resolution infrared jet-cooled study and theoretical SF_6-Rg distances calculated from RI-DFT-D *ab initio* method and from combining rules for intermolecular distances.

	R(Å)	β(Å^{-1})	$\Delta\nu_{exp}$(cm^{-1})	$\Delta\nu_{exp}\dfrac{R^6}{C_6}$	ε(cm^{-1})	$3\beta/R$
SF_6-Ne	3.90[a]	4.411	-0.117(10)	-1.35^{-3}	94.5	3.394
SF_6-Ar	4.208(5)	4.065	-0.723(1)	-4.24^{-3}	185.5	2.898
SF_6-Kr	4.341(3)	3.949	-0.981(1)	-4.92^{-3}	217.3	2.728
SF_6-Xe	4.562(1)	3.816	-1.305(1)	-5.93^{-3}	242.1	2.510

[a]The SF_6-Ne bond length was derived from the combining rule $R^{AB} \approx (R^{AA} + R^{BB})/2$ for the distances.

Table 4: Parameters used in the model of Buckingham potential for the rare gas- SF_6 heterodimers.

References

[1] M. Rossi, W. Fang and A. Michaelides, J. Phys. Chem. Lett. 6, 4233 (2015).

[2] J. S. Muenter, *in* ''Atomic and Molecular Beam Methods'' (G. Scoles, Ed.), Vol. 2. Oxford University Press, Oxford, 1995.

[3] A. C. Legon, *in* ''Atomic and Molecular Beam Methods'' (G. Scoles, Ed.), Vol. 2. Oxford University Press, Oxford, 1995.

[4] D.W.Pratt, Annu. Rev. Phys. Chem. 49,481 (1998).

[5] B.J. Howard and A.S. Pine, Chern. Phys. Lett.. 122, 1 (1985).

[6] G. T. Fraser and A. S. Pine, J. Chem. Phys. 85, 2502 (1986).

[7] D. T. Anderson, S. Davis and D. J. Nesbitt, J. Chem. Phys. 107, 1115 (1997).

[8] Z. S. Huang, K. W. Jucks and R. E. Miller , J. Chem. Phys. 85, 6905 (1986).

[9] R. W. Randall, M. A. Walsh, and B. J. Howard, Faraday Discuss. Chem. Soc. 85, 13 (1988) .

[10] G. T. Fraser, A. S. Pine, and R. D. Suenram, J. Chem. Phys. 88, 6157 (1988)

[11] M. Iida, Y. Ohshima, and Y. Endo, J. Chem. Phys. 97, 357 (1993) .

[12] T. A. Hu, E. L. Chappell, and S. W. Sharpe, J. Chem. Phys. 89, 6162 (1993).

[13] W. A. Herrebout, H-B Qian, H. Yamaguchi and B. J. Howard, J. Mol. Spectrosc. 189, 235 (1998).

[14] G. D. Hayman, J. Hodge, B. J. Howard, J. S. Muenter, and T. R. Dyke, J. Chem. Phys. 86, 1670 (1987).

[15] Y. Xu and M. C. L. Gerry, J. Mol. Spectrosc. 169, 181 (1995) .

[16] R. Lascola and D. J. Nesbitt, J. Chem. Phys. 95, 7917 (1995).

[17] X. Liu and Y. Xu, J. Mol. Spectrosc. 301, 1 (2014).

[18] G. T. Fraser, A. S. Pine and W. A. Kreiner, J. Chem. Phys. 94, 7061 (1991).

[19] P. Asselin, Y. Belkhodja, A. Jabri, A. Potapov, J. Loreau and A. van der Avoird, Mol. Phys. DOI: 10.1080/00268976.2018.1471533 (2018).

[20] T. E. Gough, D.G. Knight and G. Scoles, Chem. Phys. Lett. 97, 155 (1983).

[21] X.J. Gu, D. J. Levandier, B. Zhang, G. Scoles and D. Zhuang, J. Chem. Phys. 93 4898 (1990).

[22] R-D. Urban, L. G. Jörissen, Y. Matsumoto and M. Takami, J. Chem. Phys. 103 3960 (1995).

[23] M. Hartmann, R. E. Miller, J. P. Toennies and A. F. Vilesov, Science, 272, 1631 (1996).

[24] P. Asselin, A. Potapov, A. C. Turner, V. Boudon, L. Bruel, M-A. Gaveau, M. Mons, Phys. Chem. Chem. Phys. 19, 17224 (2017).

[25] P. Asselin, Y. Berger, T. R. Huet, R. Motiyenko, L. Margulès, R. J. Hendricks, M. R. Tarbutt, S. Tokunaga, B. Darquié, Phys. Chem. Chem. Phys. 19, 4576 (2017).

[26] M. D. Brookes, C. Xia, J. A. Anstey, B. G. Fulsom, K.-X. Au Yong, J. M. King and A. R. W. McKellar, Spectrochim. Acta, Part A, 60, 3235 (2004).

[27] Ch. J. Borde´, M. Ouhayoun, A. van Lerberghe, C. Salomon, S. Avrillier, C. D. Cantrell, and J. Borde´, Laser Spectroscopy 4, edited by H. Walther and K. W. Rothe ~Springer, New York, 1979.

[28] S. Grimme, J. Comput. Chem., 27, 1787 (2006).

[29] TURBOMOLE V6.4 2012, a development of University of Karlsruhe and Forschungszentrum Karlsruhe GmbH, 1989–2007, TURBOMOLE GmbH, since 2007; available from http://www.turbomole.com.

[30] R. A. Aziz and M. J. Slaman, Chem. Phys. 130, 187 (1989).

[31] R. A. Aziz, J. Chem. Phys. 99, 4518 (1993).

[32] A. K. Dham, A. R. Allnatt, W. J. Meath, and R. A. Aziz, Mol. Phys. **67**,1291 (1991).

[33] A. K. Dham, W. J. Meath, A. R. Allnatt, R. A. Aziz, and M. J. Slaman, Chem. Phys. 142, 173 (1990).

[34] H. A Lorentz, Ann. Physik 12, 127 (1881).

[35] R,J. Good and C.J. Hope, J. Chem.. Phys. 55, 111 (1971).

[36] R. A. Aziz, M. J. Slaman, W. L. Taylor et J. J. Hurly, J. Chem. Phys. 94, 1034 (1991).

[37] D. Eichenauer and R. J . Le Roy, J. Chem. Phys. 88, 2898 (1988).

[38] T. A. Beu, Y. Okada and K. Takeuchi, Eur. Phys. J. D. 6, 99 (1999).

[39] A. J. Stone, ''The Theory of Intermolecular Forces,'' Clarendon Press, Oxford, 1996.

[40] M. J. Seaton, Rep. Prog. Phys. 46, 167 (1983) .

[41] D. R. Lide and H. P. R. Frederikse, 77th ed. CRC, Boca Raton, FL, 1996–1997.

[42] R. T. Pack, J. J. Valentini and J. B. Cross, J. Chem. Phys. 77, 5486 (1982).

[43] R. T. Pack, J. Phys. Chem. 86, 2794 (1982).

[44] J. Tao, J. P. Perdew and A. Ruzsinszky, PNAS, 109, 18 (2012).

[45] O. A. Vydrov and T. van Voorhis, Phys. Rev. A 81, 062708 (2010).

[46] A. Kumar and W. J. Meath, Mol. Phys. 54, 823 (1985).